

SIMULATION ANALYSIS OF THE SPLASH LUBRICATION OF THE MAIN GEARBOX FOR UNMANNED HELICOPTERS

Yang, S. F.^{*,**}; Shui, J. F.^{*}; Yu, H. Y.^{**}; Wang, F.^{***}; Xu, W. B.^{***} & Xu, Y. H.^{*}

^{*} School of Intelligent Mechatronics Engineering (School of Industrial Design),
Zhongyuan University of Technology, Zhengzhou 450007, China

^{**} Weihua Group Co., Ltd., Xinxiang 453400, China

^{***} ZRIME Gearing Technology Co., Ltd, Zhengzhou 450052, China

E-Mail: yangshufeng8610@163.com

Abstract

The main gearbox of unmanned helicopters operates under complex, high-speed, and variable conditions, making lubricating oil behaviour under splash lubrication difficult to characterize and churning power loss mechanisms unclear. In this study, a computational fluid dynamics (CFD) model of the main gearbox was established to investigate lubricant flow behaviour and power dissipation in the helicopter main transmission. In particular, a numerical model was built via the moving particle semi-implicit (MPS) method. The distribution pattern of the lubricating oil in the gearbox, and the characteristics of the churning power loss under different conditions were evaluated. Results demonstrate that lubrication characteristics are influenced by the splashing effect caused by gear rotation and the fluidity of the lubricant. Churning power loss increases with gear speed and initial oil quantity, while it decreases as lubricating oil temperature rises, exhibiting a nonlinear trend overall. The proposed method provides a theoretical basis for optimizing the splash lubrication scheme and improving the energy efficiency of the main gearbox of unmanned helicopters.

(Received in October 2025, accepted in January 2026. This paper was with the authors 2 weeks for 2 revisions.)

Key Words: Main Gearbox, Unmanned Helicopters, Moving Particle Semi-Implicit Method, Splash Lubrication, Churning Power Loss

1. INTRODUCTION

The main gearbox, considered a key functional component in power transmission systems of unmanned helicopters, undertakes the core tasks of power transmission and speed conversion. The operational safety and reliability of the main gearbox directly determine the flight safety and service life of the whole machine. Splash lubrication, a method known for its high power density, compact structure layout, and complex service environment, is generally adopted for the main gearbox of helicopters to achieve effective lubrication and cooling of gear meshing pairs and bearings in limited space. However, under high-speed operation, splash lubrication inevitably introduces significant churning power loss. In addition, a considerable part of the energy eventually accumulates in the gearbox in the form of heat. These issues restrict the transmission efficiency and thermal safety performance of splash lubrication.

From the perspective of the power loss mechanism, gearbox power dissipation is generally classified into two categories: load-related losses and losses independent of load; among them, churning loss constitutes the primary component of the load-independent part and becomes dominant under high-speed operating conditions [1]. Unlike tooth surface friction loss, churning loss is governed by local contact behaviour as well as by gear speed, geometric features, and the transient oil distribution within the gearbox. In essence, churning loss originates from a highly unsteady and strongly nonlinear multiphase flow process. As lubricating oil presents complex spray, splash, and backflow behaviour under gear rotation and meshing, the spatial distribution and momentum exchange of lubricating oil cannot be accurately described via simplified assumptions. This issue leads to long-term significant uncertainty in the mechanism cognition and quantitative prediction of churning loss. In

engineering practice, the churning loss is assessed mostly via tests or empirical correlation models [2, 3]. Despite the ability to reflect the loss level under specific structures or working conditions, the applicability of this technique is restricted by testing conditions and model assumptions, hindering its promotion in helicopters' real-world main gearbox system. Furthermore, the main gearbox system is geometrically complicated and highly coupled in terms of operating parameters. Unmanned helicopters have continuously acquired advanced high-speed and lightweight features in highly reliable research directions. Consequently, traditional empirical methods can no longer fully satisfy engineering design needs in terms of efficiency prediction accuracy.

The discussion presented above shows that fundamental research has been conducted on the splash lubrication mechanism of helicopter gearboxes and their churning power loss. However, simplified geometry and working conditions have mostly been employed, hindering the full understanding of the coupling relationship between the distribution of lubricating oil and the churning power loss in real structures. A problem to be solved urgently lies in accurately revealing the lubricating oil distribution characteristics under splash lubrication and their influencing mechanism on churning power loss while retaining the geometry–meshing relationship of real gears. In this study, with an unmanned helicopter's main gearbox as the study object, a three-dimensional numerical model was established. The influences of factors including rotational velocity, initial oil quantity, and temperature of the oil, on lubrication performance and churning power loss were systematically examined using the MPS method.

2. STATE OF THE ART

The splash lubrication behaviour of gearboxes and their churning power loss have been extensively investigated by Chinese and foreign scholars. Early research focused on tests, and the basic motion form of lubricating oil and its relationships with speed and geometric parameters were revealed via visualization or power measurement. Leprince et al. [4] qualitatively analysed the spray and splash behaviour of lubricating oil under different rotational speeds and geometric conditions on the basis of a single-gear churning test bench, providing an experimental basis for the subsequent study of mixing loss. Changenet and Vexex [5] built a special gear test bench, systematically studied the flow characteristics and power loss of splash lubrication under different structural configurations, and adopted several semi-empirical prediction models. Polly et al. [6] quantified the contributions of gear resistance, the meshing cavity effect, and the relationship between bearings and the total rotation loss via separate loss tests of single gears and gear pairs; however, limitations were evident in terms of cost, repeatability, and parameter expansion ability, and the complex and changeable operating conditions in practical engineering were overlooked.

With the advancement of CFD [7, 8], the finite volume method (FVM) has gradually become an important tool for investigating gearbox lubrication and churning loss. Liu et al. [9] developed an FVM-based numerical gearbox model and, in combination with experimental data, validated the effects of lubricant viscosity and rotational speed on churning loss. Hu et al. [10] introduced the dynamic motion of gears and systematically analysed the effects of rotational speed, lubricant performance, and structural parameters on churning power loss. Mastrone and Concli [11] predicted the efficiency and power loss of a multistage reducer via multizone grid technology and achieved good experimental consistency. In general, the FVM method is a mature technique for describing lubricating oil diffusion and macrochurning loss; however, as the FVM is based on the fixed-grid Euler description framework, the geometric model should be simplified or zoomed in when dealing with large deformation movement and complex free liquid surface problems in the gear meshing zone [12]. This issue weakens the

representativeness of simulation results for real engineering structures. Consequently, the limitations of grid-based methods in geometric processing and free surface tracking were addressed by adopting particle methods based on Lagrange descriptions. Among them, smooth particle hydrodynamics (SPH) and MPS methods represent fluid media by discrete particles. These methods can naturally capture the splashing, crushing, and re-combination processes of lubricating oil without complex mesh division. Ji et al. [13] established a multiphase flow model of a gearbox via the SPH method and verified its advantages via local flow field analysis and by comparing it with PIV test results. Legrady et al. [14] applied the SPH method to simulate the flow field in a bevel gear transmission box. Although this scheme performed well in reproducing the flow pattern, it still had shortcomings in terms of the prediction accuracy of power loss, which was also verified by Liu et al. [15]. Conversely, the MPS method has demonstrated high stability and accuracy in addressing lubricant behaviour and predicting churning loss under high Reynolds numbers [16]. Wei et al. [17] employed the MPS method to hydraulic systems of engineering vehicles and achieved a good balance between geometric authenticity and computational feasibility in complex engineering structures. Shao et al. [18] extended the MPS approach to the gearbox of high-speed trains and systematically revealed the influence of multiple operating parameters affect the distribution of lubricating oil and churning loss. These studies demonstrated that MPS exhibits clear advantages for the accurate prediction of churning loss in gear transmission systems.

In helicopter main gearbox research, as the intersecting-shaft bevel drive is generally adopted, the internal oil movement is more complex because of its variable speed angle and spatial layout. Lu et al. [19] established an oil-gas two-phase flow model of a helicopter reducer via the CFD method and analysed the transport mechanism and thermal behaviour of the lubricant via the MRF method. Hu et al. [20] systematically studied the influence of multiple operating parameters on churning loss in view of the splash lubrication problem of a spiral bevel gear pair. However, most of the studies have been based on idealized or simplified geometric models. These issues have hindered the understanding of the geometrical characteristics of real tooth surfaces, meshing relations, and multiparameter coupling effects, further limiting the engineering guidance value of numerical results.

The abovementioned studies also focused mainly on analysing the fundamental flow behaviour of lubricant, together with the factors affecting churning power dissipation under splash-lubricated conditions. However, under the real geometric conditions of gearboxes, the formation mechanism of churning loss under the joint action of multiple operating parameters has not been fully investigated. With respect to maintaining the authenticity of gear geometry and motion, the internal relationship between lubricant distribution characteristics and churning power dissipation has been quantitatively described in few studies. In this study, a three-dimensional main gearbox model, used to investigate the real gear geometry-meshing relation, was established on the basis of the MPS method. The movement behaviour of lubricating oil under splash lubrication and its influence on churning power loss were systematically identified. The aim of this study was to provide a theoretical basis for predicting losses in the main gearbox of unmanned helicopters and the optimization of structural and lubrication schemes.

The remainder of this study is organized as follows. Section 3 presents the MPS method, the formulation for churning loss, and the development of the main gearbox and numerical models. Section 4 presents the numerical calculation results and analyses of the complex working conditions of the gearbox and the effects of operating parameters on lubrication and churning loss. Section 5 summarizes the study and presents relevant conclusions.

3. METHODOLOGY

3.1 Basic introduction to MPS

The MPS method expresses fluid as a set of discrete particles and tracks the movement of such particles via the Lagrangian framework. The continuity equation and Navier–Stokes equation serve as the basic governing equations for fluid movement in the MPS method [21].

The continuity equation is expressed as:

$$\frac{d\rho}{dt} = 0 \quad (1)$$

and the Navier–Stokes equation is given by:

$$\frac{du}{dt} = -\frac{\nabla p}{\rho} + \nu \nabla^2 u + f \quad (2)$$

where ρ is the fluid density, u is the velocity vector, p stands for pressure, ν is the kinematic coefficient of viscosity, f denotes the gravitational acceleration, and t represents time.

In the MPS framework, interparticle interactions are weighted using a kernel function [22]. When $r_{ij} \leq r_e$, the particles interact with each other, and the influence decreases with increasing distance. When $r_{ij} > r_e$, the interactions between particles cannot be observed. The kernel function is mathematically defined as follows:

$$w(r_{ij}) = \begin{cases} \frac{r_e}{r_{ij}} - 1 & (r_{ij} \leq r_e) \\ 0 & (r_{ij} > r_e) \end{cases} \quad (3)$$

where r_{ij} represents the distance between particles i and j , and r_e defines the radius of action, which designates the maximum range of effective particle interactions.

In the MPS framework, the number density represents particle distribution within a specified neighbourhood. The number density of particle is obtained by evaluating the kernel function as follows [23]:

$$n_i = \sum_{j \neq i} w(r_{ij}) \quad (4)$$

where n_i is the particle number density.

The fluid velocity and pressure fields in the MPS method are primarily governed by the gradient and Laplacian models. The gradient model, together with the Laplace model [24], is expressed as follows:

$$\nabla \eta_i = \frac{d}{n^0} \sum_{j \neq i} \frac{\eta_j - \eta_i}{|\mathbf{r}_j - \mathbf{r}_i|^2} (\mathbf{r}_j - \mathbf{r}_i) W(|\mathbf{r}_j - \mathbf{r}_i|) \quad (5)$$

$$\nabla^2 \eta_i = \frac{2d}{\lambda n^0} \sum_{j \neq i} (\eta_j - \eta_i) W(|\mathbf{r}_j - \mathbf{r}_i|) \quad (6)$$

$$\lambda = \frac{\sum_{j \neq i} w(r_{i,j}) |\mathbf{r}_j - \mathbf{r}_i|^2}{\sum_{j \neq i} w(r_{i,j})} \quad (7)$$

where η denotes a scalar particle parameter, r_i and r_j represent the position vectors, d represents the spatial dimensionality, n^0 denotes a particle number density constant, and λ represents the Laplace coefficient.

The accurate identification of free surfaces is highly important for ensuring the accuracy of numerical calculations. According to the physical properties of the fluid, the particle density outside the free surface should be lower than that inside the fluid. When the local particle density is lower than the threshold, this particle is identified as a free surface particle. Free surface particles are determined as follows [25]:

$$n_i^* < \beta n^0 \quad (8)$$

where β is the discriminant parameter, whose recommended range is $0.8 \leq \beta < 1$. In this study, β takes a value of 0.97.

Besides addressing free-surface boundary conditions, the MPS method relies on the accurate identification of solid boundaries. In general, solid boundary particles are divided into three layers [26] (Fig. 1). The outermost layer consists of fluid-interface particles for pressure calculations, while solid particles in the two internal layers are used to calculate particle density and stabilize the boundary.

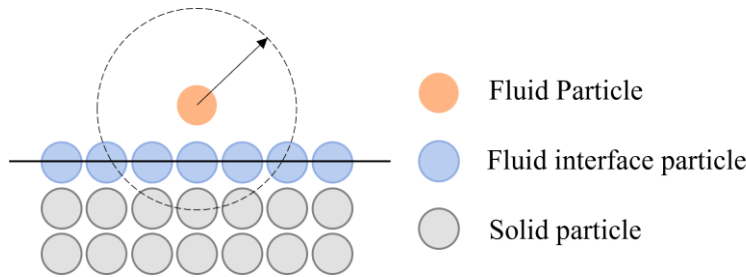


Figure 1: Layout of boundary particles.

In the MPS method, the hydrodynamic force acts upon the tooth surface via interpolation, and the tooth surface is subjected to a counteracting force, i.e., the oil churning resistance. As revealed by multiple studies, this resistance can be divided into three main types: the first type derives from the pressure gradient effect; the second type originates from the viscous force generated when lubricating oil is stirred by the gear; and the third type derives from the shear stress related to the turbulence phenomenon. The resistance is calculated as follows [27]:

$$\langle \nabla p \rangle_i = \frac{d}{n^0} \sum_{j \neq i} \left[\frac{p_j - \hat{p}_i}{|\mathbf{r}_j - \mathbf{r}_i|^2} (\mathbf{r}_j - \mathbf{r}_i) w(r_{ij}) \right] \quad (9)$$

$$\nu \nabla^2 \mathbf{u}_i = \nu \frac{2d}{\lambda n^0} \sum_{j \neq i} [(\mathbf{u}_j - \mathbf{u}_i) w(r_{ij})] \quad (10)$$

$$\tau = \rho l^2 \left| \frac{\partial \mathbf{u}}{\partial y} \right| \frac{\partial \mathbf{u}}{\partial y} \quad (11)$$

where τ represents the turbulence-induced shear stress, and l denotes the characteristic length for mixing.

The total gearbox power loss (P_{loss}) is commonly evaluated as the sum of the products of each gear's rotational torque and the corresponding angular speed. P_{loss} is mathematically expressed as follows:

$$P_{loss} = \frac{T_{loss} \times N}{9550} \quad (12)$$

where T_{loss} represents the torque of the gears generated because of the oil churning resistance, and N represents the rotational speed of the gears.

3.2 Geometry modelling and grid preprocessing

A three-dimensional model of a spiral bevel gearbox for a helicopter transmission system was established in this study. This gearbox has a single-stage gear structure, in which the output gear is driven to run by splash lubrication, i.e., the rotating input gear. The key parameters associated with the bevel gear pair are summarized in Table I.

Given the complex structure and numerous components of helicopter gearboxes, their drive mode and working principle should be combined for reasonable model simplification, improving the simulation calculation efficiency. The details are as follows:

(1) Unnecessary external components, including bolts, nuts, and screws on the helicopter surface, were simplified. The internal geometrical characteristics affecting lubrication performance were reserved.

(2) The through holes on the box body and the components extending to the axis outside the gearbox were removed so that the inner and outer box surfaces can be flatter and smoother.

Table I: Main geometric characteristics of the bevel gear.

Variable	Driving gear	Driven gear
Tooth surface type	Gleason style	
Tooth number	9	43
Module /mm	4.21	
Tooth width /mm	32	
Pressure angle /°	20	
Helix angle /°	35	

The box with particles was filled, and the MPS approach was employed to simulate the lubricating oil. Additionally, the MPS method can retain complex geometric shapes, effectively improving the authenticity of the model. Fig. 2 shows the simplified helicopter gearbox structure.

In this model, the continuous-phase lubricant is discretized into a series of lubricant particles (Fig. 3). In CFD, the particle size is one of the key factors affecting the calculation accuracy. In general, the smaller the particle size is, the higher the resolution of the flow field. However, considering the current calculation resources and time cost, the particle size of the lubricating oil is specified as 1 mm in this study.

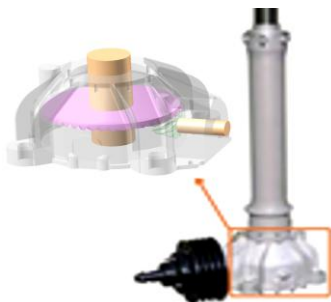


Figure 2: Simplified gearbox model.

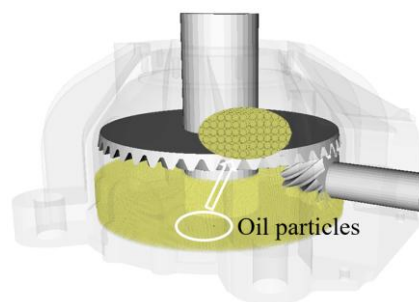


Figure 3: Oil particle model.

The Coulomb number is 0.2, the pressure and viscosity models are implicit models, and the possible model results are nearly the same. Considering the gravity of the particles in the calculation, the gravitational acceleration is 9.8 m/s^2 . Given the relatively complex fluid in the gearbox, the simulation is performed via the LES turbulence model. A suitable time step is chosen to enhance numerical stability and solution convergence; its mathematical expression is given as follows [28]:

$$\Delta t = \min \left(\Delta t_i, \frac{Cl_0}{u_{\max}}, \frac{d_i l_0^2}{2(v + v_{\max})} \right) \quad (13)$$

where Δt_i denotes the initial time step; C represents the Courant number; l_0 represents the particle diameter; u_{\max} represents the maximum particle velocity; d_i represents the diffusion coefficient; v represents the dynamic viscosity; and v_{\max} represents its maximum value. The Courant–Friedrichs–Lewy (CFL) criterion [28] should be satisfied, thereby ensuring the computational stability of viscosity conditions.

This helicopter gearbox is lubricated and cooled with 75 W-90 oil. The properties of this lubricant are listed in Table II. Combining AGMA’s viscosity–temperature formula [29], the viscosity–temperature relationship for the lubricant is given, and the density–temperature relationship is approximately fitted. A and B are constants.

$$\lg[\lg(v + 0.7)] = A - B \lg(\theta + 273.15) \quad (14)$$

$$\rho = 876 - 0.6\theta \quad (15)$$

where ρ represents the density of the lubricating oil, kg/m^3 ; θ represents the temperature, $^\circ\text{C}$; and v represents the kinematic viscosity, mm^2/s .

Table II: Basic characteristics of the 75 W-90 lubricating oils.

Parameter	Value	Test method
Density at 15 °C /(kg/m ³)	867	DIN 51757
Kinematic viscosity at 40 °C /(mm ² /s)	116	ASTM D445
Kinematic viscosity at 100 °C /(mm ² /s)	16.6	ASTM D445

Table III presents 10 numerical simulation tests to compare the influence of speed, initial oil quantity, and temperature on gearbox lubrication. Conditions 1 to 4 are applied to examine the effect of speed variation; Conditions 3, 5 to 7 are employed to investigate the effect on the initial amount of lubricating oil quantity; and Conditions 3, 8 to 10 are used to study the influence of ambient temperature. The simulation lasted for 1 second. The acceleration stage lasted for 0 to 0.15 s, and the steady-state stage lasted for 0.15 to 1 s.

Table III: Simulation conditions.

Simulation model	Driving gear rotation speed (rpm)	Initial oil volume (L)	Temperature (°C)
G1	1600	18	40
G2	2400	18	
G3	3200	18	
G4	4000	18	
G5	3200	15	
G6	3200	21	
G7	3200	24	
G8	3200	15	0
G9	3200	15	20
G10	3200	15	60

4. SIMULATION ANALYSIS AND DISCUSSION

4.1 Effect of gear speed on lubrication performance

The gear speed affects the lubrication effect and the running state of the gear. The viscosity of the lubricant usually decreases. Figs. 4 and 5 show the isograms of lubricant particle density

and velocity fields at different gear speeds for a moderate quantity of low-viscosity lubricating oil, respectively. The results show that the lubricant particles in the gearbox at different speeds maintain a consistent overall distribution trend, and the particles generated by churning are mainly concentrated near the driven gear. At a speed of 1600 r/min, most of the lubricant is attached to the gear tooth surface, whereas splashed oil drops tend to gather beneath and behind the shell. As the speed accelerates, the centrifugal force increases, leading to an increase in oil quantity and a more evident splashing phenomenon. At 4000 r/min, the lubricant intensely splashes to the meshing surface and the inner surface of the shell, indicating a larger contact area under high-speed operation.

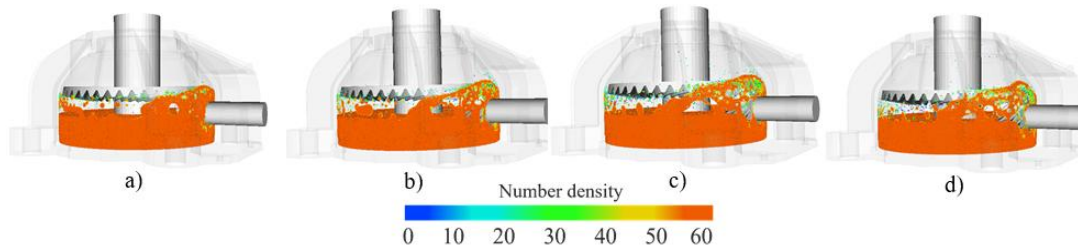


Figure 4: Lubricant particle density distributions at different speeds: a) 1600 rpm, b) 2400 rpm, c) 3200 rpm, and d) 4000 rpm.

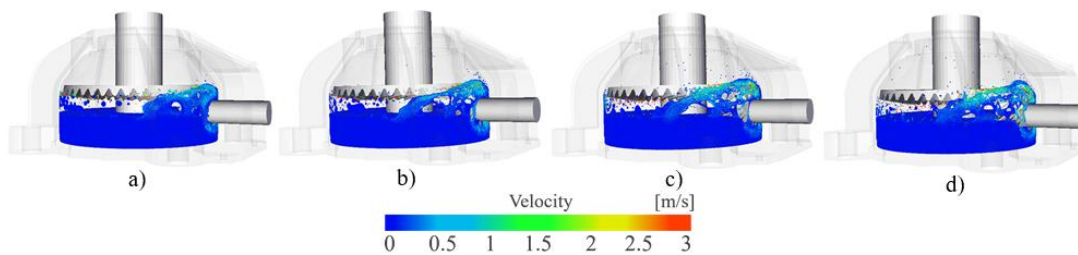


Figure 5: Lubricant particle velocity changes at different gear speeds: a) 1600 rpm, b) 2400 rpm, c) 3200 rpm, and d) 4000 rpm.

4.2 Effect of initial oil quantity on lubrication performance

The quantity of oil added into the gearbox plays a crucial role in its operation and the internal flow and dispersion. Figs. 6 and 7 show the lubricating oil distribution under different initial oil quantities. The results indicate that with increasing initial oil quantity, the number of oil drops generated by gear churning increases, further raising the total concentration of oil within the gearbox. The greater the initial oil quantity, the more pronounced this trend becomes. At a low oil quantity, an appropriate increase in the oil quantity improves the churning and circulation of the oil; at a high oil quantity, a substantial increase in the oil quantity increases the churning intensity. An increase in splashing allows the lubricating oil to be distributed more evenly, ultimately increasing the total concentration of lubricating oil and further increasing the average concentration.

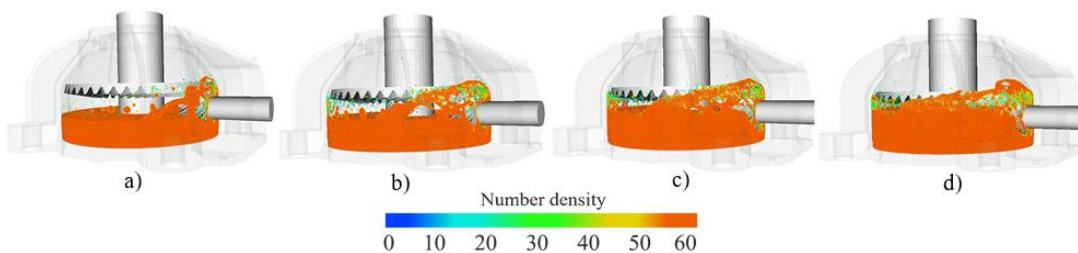


Figure 6: Lubricating oil particle density distributions for different initial oil quantities: a) 15 L, b) 18 L, c) 21 L, and d) 24 L.

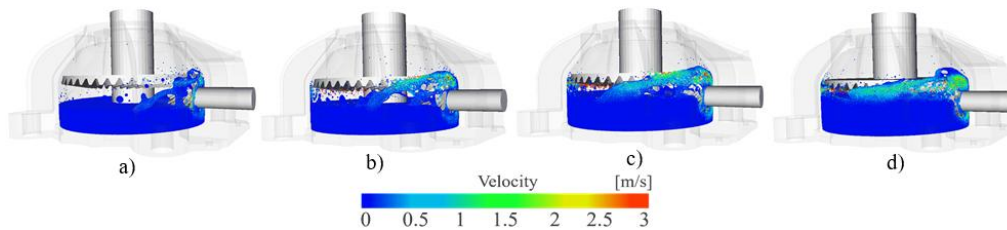


Figure 7: Velocity changes in lubricating oil particles under different initial oil quantities: a) 15 L, b) 18 L, c) 21 L, and d) 24 L.

4.3 Effects of oil temperature on lubrication performance

Gear rotation produces significant disturbances, wind resistance, and meshing loss, which jointly increase the power loss and lubricating oil temperature. The rising oil temperature decreases the oil viscosity and improves its liquidity, further changing the lubricating state. Figs. 8 and 9 show the changes in the lubricating oil particle density distribution and velocity field at different oil temperatures and a gear speed of 3200 r/min. At a low temperature, the lubricating tension is weak, and oil particles are densely gathered around the gear surface, forming a stable lubricating oil film with improved lubrication. However, given the limited oil splash capacity, the majority of the oil still accumulates near the base of the gearbox, leading to a relatively concentrated distribution of the internal oil phase and a low overall lubricating oil density. As the temperature increases, the oil viscosity decreases, the oil liquidity improves, and the driving force formed by the gear to lubricate the oil is strengthened. Consequently, more oil drops are splashed, increasing the quantity of oil within the gearbox. This change becomes noticeable at reduced temperatures. Once the oil temperature surpasses 40 °C, given the temperature-dependent change in viscosity, the effect of thermal changes on lubrication performance is weakened. At low temperatures, the viscosity changes rapidly with temperature. With the oil temperature rising from 0 °C to 20 °C, the viscosity decreases to one-fourth of the initial value. As the oil temperature rises further from 40 °C to 60 °C, the viscosity decreases by approximately 43 %. This trend indicates that the viscosity changes slowly with increasing temperature.

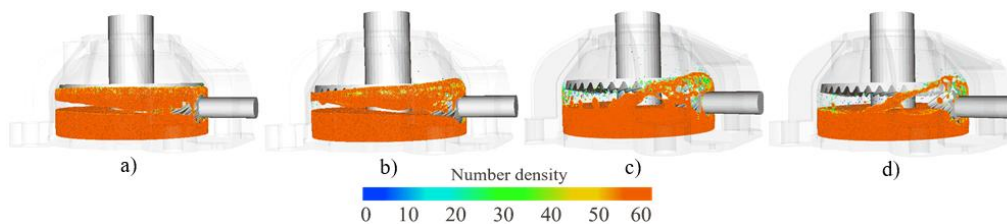


Figure 8: Lubricant particle density distributions at different temperatures: a) 0 °C, b) 20 °C, c) 40 °C, and d) 60 °C.

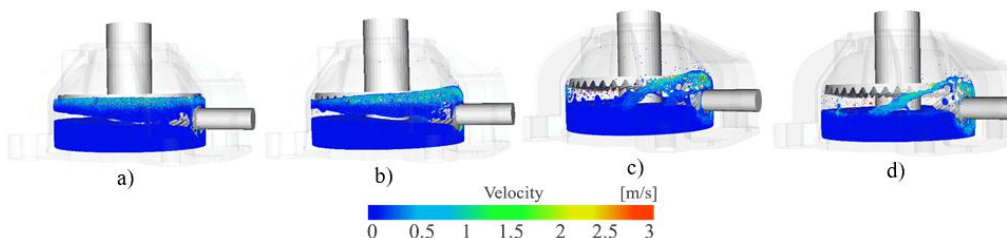


Figure 9: Changes in particle velocity with temperature: a) 0 °C, b) 20 °C, c) 40 °C, and d) 60 °C.

4.4 Churning loss analysis

In the running process, the gearbox subject to splash lubrication undergoes meshing friction loss, wind resistance loss, and churning loss. The churning loss constitutes roughly 30 % of

the total energy dissipation of the gearbox. Hence, reducing the churning loss is not only helpful in reducing the overall energy consumption of the gearbox but can also significantly improve its transmission efficiency and lengthen its service life. In this study, the churning loss torque of the gear under each operating condition was calculated, and the impacts of 10 conditions on the churning loss of the gear pair were analysed.

The average churning torque in the time interval of 0.8–1 s was considered as the churning torque. The power loss due to oil churning in the gear pair under various operating conditions was computed using the Eq. (12). As shown in Fig. 10, the churning power loss gradually increases with increasing gear speed and initial lubricating oil quantity. Furthermore, the churning power loss decreases with increasing oil temperature. Notably, the churning power loss is highly sensitive to gear speed; particularly under high-speed operating conditions, it increases markedly with increasing gear speed. Given the relatively high viscosity of lubricating oil at low temperatures, its flow characteristics are significantly different from those at room temperature, increasing the flow resistance and generating high churning power loss.

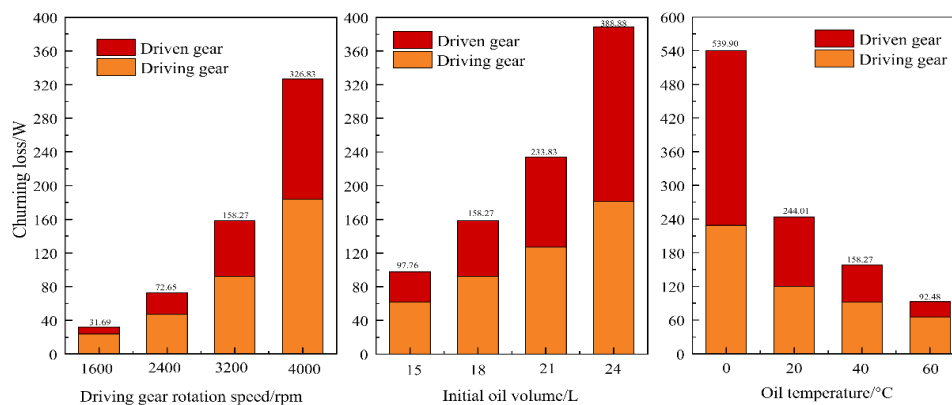


Figure 10: Churning power loss for various numerical models.

5. CONCLUSION AND FUTURE WORK

In this study, the main gearbox of a helicopter was chosen as the subject, its structural features were appropriately simplified, and a 3D CFD simulation model was developed. The lubrication behaviour inside the gearbox was visualized using the MPS approach. Ten CFD simulations were performed, and the impacts of the gear rotation direction, speed, initial oil quantity, and temperature on the distribution of lubricating oil and churning power loss were examined. The main conclusions are summarized as follows:

(1) The splash lubrication behaviour of the helicopter's main gearbox were subjected to visual simulation via the MPS method. Combined with fluid visualization analysis, the MPS method can improve the ability to predict lubricating fluid movement and power loss in the gearbox. This finding provides a new research path for the quantitative evaluation and optimization of lubrication performance.

(2) Visualization analysis was performed on the density of lubricating fluid particles and velocity spread inside the gearbox under different gear speeds, initial oil quantity, and oil temperatures. The results indicated that the lubrication behaviour of the gearbox is primarily influenced by the splash behaviour caused by gear rotation and the fluid flow characteristics. Among them, the gear speed and initial oil quantity are the key factors influencing the strength of the oil splash. Lubricant temperature has a considerable impact on its flow characteristics.

(3) The churning power loss caused by gear oil churning under different working conditions was calculated, and its variation was systematically analysed. The results showed

as the gear speed and initial amount of lubricating fluid increase, the churning power loss significantly increases. As the lubricating oil temperature increases, the viscosity, fluidity, and churning resistance of the oil decreases, and the churning power loss gradually decreases. In general, the churning power loss of gear oil clearly exhibits nonlinear characteristics with changes in speed, initial oil quantity, and oil temperature.

The close internal relationships among the gear speed and the viscosity and temperature of lubricating oil have been widely recognized. Increasing speed aggravates gear churning and friction-induced heat, reduces the viscosity of the lubricating oil, and changes its distribution characteristics inside the gearbox. In this study, the abovementioned parameters were analysed separately. The objectives were to analyse the main effects of the parameters on splash lubrication behaviour and establish a preliminary understanding of the related physical mechanism. In future research, a completely coupled thermal fluid simulation framework will be built to describe in detail the interaction and coupling effects among different factors.

ACKNOWLEDGEMENT

The study was supported by the National Natural Science Foundation of China (No. U52075561).

REFERENCES

- [1] Michaelis, K.; Höhn, B.-R.; Hinterstoißer, M. (2011). Influence factors on gearbox power loss, *Industrial Lubrication and Tribology*, Vol. 63, No. 1, 46-55, doi:[10.1108/00368791111101830](https://doi.org/10.1108/00368791111101830)
- [2] Changenet, C.; Velex, P. (2007). A model for the prediction of churning losses in geared transmissions – preliminary results, *Journal of Mechanical Design*, Vol. 129, No. 1, 128-133, doi:[10.1115/1.2403727](https://doi.org/10.1115/1.2403727)
- [3] Seetharaman, S.; Kahraman, A.; Moorhead, M. D.; Petry-Johnson, T. T. (2009). Oil churning power losses of a gear pair: experiments and model validation, *Journal of Tribology*, Vol. 131, No. 2, Paper 022202, 10 pages, doi:[10.1115/1.3085942](https://doi.org/10.1115/1.3085942)
- [4] Leprince, G.; Changenet, C.; Ville, F.; Velex, P. (2012). Investigations on oil flow rates projected on the casing walls by splashed lubricated gears, *Advances in Tribology*, Vol. 2012, No. 1, Paper 365414, 7 pages, doi:[10.1155/2012/365414](https://doi.org/10.1155/2012/365414)
- [5] Changenet, C.; Velex, P. (2008). Housing influence on churning losses in geared transmissions, *Journal of Mechanical Design*, Vol. 130, No. 6, Paper 062603, 6 pages, doi:[10.1115/1.2900714](https://doi.org/10.1115/1.2900714)
- [6] Polly, J.; Talbot, D.; Kahraman, A.; Singh, A.; Xu, H. (2018). An experimental investigation of churning power losses of a gearbox, *Journal of Tribology*, Vol. 140, No. 3, Paper 031102, 8 pages, doi:[10.1115/1.4038412](https://doi.org/10.1115/1.4038412)
- [7] Feng, Y. T.; Peng, J. S.; Tang, Z. S.; Yang, X.; Huang, W. (2025). CFD-experimental study on thermoflow in rice huller chamber, *International Journal of Simulation Modelling*, Vol. 24, No. 3, 509-520, doi:[10.2507/IJSIMM24-3-CO12](https://doi.org/10.2507/IJSIMM24-3-CO12)
- [8] Wang, J.; Zhang, J. R.; Liu, X. L. (2025). CFD simulation of wind-rain effects on ultra-high-speed train aerodynamics and safety, *International Journal of Simulation Modelling*, Vol. 24, No. 4, 706-717, doi:[10.2507/IJSIMM24-4-CO18](https://doi.org/10.2507/IJSIMM24-4-CO18)
- [9] Liu, H.; Jurkschat, T.; Lohner, T.; Stahl, K. (2018). Detailed investigations on the oil flow in dip-lubricated gearboxes by the finite volume CFD method, *Lubricants*, Vol. 6, No. 2, Paper 47, 14 pages, doi:[10.3390/lubricants6020047](https://doi.org/10.3390/lubricants6020047)
- [10] Hu, X.; Wang, A.; Li, P.; Wang, J. (2021). Influence of dynamic attitudes on oil supply for bearings and churning power losses in a splash lubricated spiral bevel gearbox, *Tribology International*, Vol. 159, Paper 106951, 16 pages, doi:[10.1016/j.triboint.2021.106951](https://doi.org/10.1016/j.triboint.2021.106951)
- [11] Mastrone, M. N.; Concli, F. (2022). A multi-domain modeling approach for the CFD simulation of multi-stage gearboxes, *Energies*, Vol. 15, No. 3, Paper 837, 16 pages, doi:[10.3390/en15030837](https://doi.org/10.3390/en15030837)
- [12] Santra, T. S.; Raju, K.; Deshmukh, R.; Gopinathan, N.; Paradarami, U.; Agrawal, A. (2019). *Prediction of Oil Flow Inside Tractor Transmission for Splash Type Lubrication*, SAE Technical Paper 2019-26-0082, SAE International, Warrendale, 7 pages, doi:[10.4271/2019-26-0082](https://doi.org/10.4271/2019-26-0082)

- [13] Ji, Z.; Stanic, M.; Hartono, E. A.; Chernoray, V. (2018). Numerical simulations of oil flow inside a gearbox by Smoothed Particle Hydrodynamics (SPH) method, *Tribology International*, Vol. 127, 47-58, doi:[10.1016/j.triboint.2018.05.034](https://doi.org/10.1016/j.triboint.2018.05.034)
- [14] Legrady, B.; Taesch, M.; Tschirschnitz, G.; Mieth, C. F. (2022). Prediction of churning losses in an industrial gear box with spiral bevel gears using the smoothed particle hydrodynamic method, *Forschung im Ingenieurwesen*, Vol. 86, No. 3, 379-388, doi:[10.1007/s10010-021-00514-6](https://doi.org/10.1007/s10010-021-00514-6)
- [15] Liu, H.; Arfaoui, G.; Stanic, M.; Montigny, L.; Jurkschat, T.; Lohner, T.; Stahl, K. (2019). Numerical modelling of oil distribution and churning gear power losses of gearboxes by smoothed particle hydrodynamics, *Proceedings of the Institution of Mechanical Engineers, Part J: Journal of Engineering Tribology*, Vol. 233, No. 1, 74-86, doi:[10.1177/1350650118760626](https://doi.org/10.1177/1350650118760626)
- [16] Guo, D.; Chen, F.; Liu, J.; Wang, Y.; Wang, X. (2020). Numerical modeling of churning power loss of gear system based on moving particle method, *Tribology Transactions*, Vol. 63, No. 1, 182-193, doi:[10.1080/10402004.2019.1682212](https://doi.org/10.1080/10402004.2019.1682212)
- [17] Wei, C.; Wu, W.; Hou, X.; Nelias, D.; Yuan, S. (2023). Research on flow pattern of low temperature lubrication flow field of rotating disk based on MPS method, *Tribology International*, Vol. 180, Paper 108221, 10 pages, doi:[10.1016/j.triboint.2023.108221](https://doi.org/10.1016/j.triboint.2023.108221)
- [18] Shao, S.; Zhang, K.; Yao, Y.; Liu, Y.; Yang, J.; Xin, Z.; He, K. (2024). A study on the lubrication characteristics and parameter influence of a high-speed train herringbone gearbox, *Lubricants*, Vol. 12, No. 8, Paper 270, 20 pages, doi:[10.3390/lubricants12080270](https://doi.org/10.3390/lubricants12080270)
- [19] Lu, F.; Wang, M.; Bao, H.; Huang, W.; Zhu, R. (2022). Churning power loss of the intermediate gearbox in a helicopter under splash lubrication, *Proceedings of the Institution of Mechanical Engineers, Part J: Journal of Engineering Tribology*, Vol. 236, No. 1, 49-58, doi:[10.1177/13506501211010030](https://doi.org/10.1177/13506501211010030)
- [20] Hu, S.; Gong, W.; Gui, P. (2024). Numerical study on the churning power loss of spiral bevel gears at splash lubrication system, *Lubrication Science*, Vol. 36, No. 4, 259-276, doi:[10.1002/lis.1688](https://doi.org/10.1002/lis.1688)
- [21] Li, G.; Wen, P.; Feng, H.; Zhang, J.; Yan, J. (2020). Study on melt stratification and migration in debris bed using the moving particle semi-implicit method, *Nuclear Engineering and Design*, Vol. 360, Paper 110459, 15 pages, doi:[10.1016/j.nucengdes.2019.110459](https://doi.org/10.1016/j.nucengdes.2019.110459)
- [22] Zhang, K.; Sun, Z.; Xi, G. (2019). Influence of the kernel function characteristics on the stability of pressure solution of moving particle semi-implicit method, *Journal of Xi'an Jiaotong University*, Vol. 53, No. 9, 1-6
- [23] Zhao, L.; Punetha, M.; Ma, W.; Konovalenko, A.; Bechta, S. (2023). Simulation of melt spreading over dry substrates with the moving particle semi-implicit method, *Nuclear Engineering and Design*, Vol. 405, Paper 112229, 12 pages, doi:[10.1016/j.nucengdes.2023.112229](https://doi.org/10.1016/j.nucengdes.2023.112229)
- [24] Liu, X.; Morita, K.; Zhang, S. (2021). Direct numerical simulation of incompressible multiphase flow with vaporization using moving particle semi-implicit method, *Journal of Computational Physics*, Vol. 425, Paper 109911, 18 pages, doi:[10.1016/j.jcp.2020.109911](https://doi.org/10.1016/j.jcp.2020.109911)
- [25] Daneshvar, F. A.; Rakhshandehroo, G. R.; Talebbeydokhti, N. (2017). New modified gradient models for MPS method applied to free-surface flow simulations, *Applied Ocean Research*, Vol. 66, 95-116, doi:[10.1016/j.apor.2017.05.009](https://doi.org/10.1016/j.apor.2017.05.009)
- [26] Monaghan, J. J. (1994). Simulating free surface flows with SPH, *Journal of Computational Physics*, Vol. 110, No. 2, 399-406, doi:[10.1006/jcph.1994.1034](https://doi.org/10.1006/jcph.1994.1034)
- [27] Liu, H.; Wei, T.; Zhou, J.; Xie, C. (2023). Research on characteristics of splash lubrication and power losses of reducer based on MPS method, *Lubrication Science*, Vol. 35, No. 8, 596-615, doi:[10.1002/lis.1667](https://doi.org/10.1002/lis.1667)
- [28] Schneider, K.; Kolomenskiy, D.; Deriaz, E. (2012). Is the CFL condition sufficient? Some remarks, De Moura, C. A.; Kubrusly, C. S. (Eds.), *The Courant–Friedrichs–Lewy (CFL) Condition: 80 Years After Its Discovery*, Birkhäuser, Boston, 139-146, doi:[10.1007/978-0-8176-8394-8_9](https://doi.org/10.1007/978-0-8176-8394-8_9)
- [29] AGMA 925-A03 (2003). *Effect of Lubrication On Gear Surface Distress*, AGMA Information Sheet, American Gear Manufacturers Association, Alexandria, 9-10